STRESS CORROSION CRACKING OF COPPER SINGLE CRYSTALS : EXPERIMENTS AND NUMERICAL MODELLING.

J.P. Chateau*, B. Bayle* and T. Magnin*

Slow tensile tests in $NaNO_2$ were performed on <100> single crystals of pure copper. They exhibit a macroscopically brittle fracture which is discontinuous at a more microscopic scale and often composed with {111} and {110} microfacets. In accordance with these results, new developpements of the corrosion enhanced plasticity model are discussed. This model, proposed by one of the present authors some years ago, is based on an enhanced mobility of dislocations due to corrosion. The first results of a numerical simulation of the corrosion-deformation interactions at the crack tip are presented. They show the formation of a moving dislocation pile-up, inducing a local stress concentration for microcracking.

INTRODUCTION

The deleterious effect of an agressive environment on the mechanical properties of materials is well known. Many studies have shown that a discontinuous cleavage-like fracture occurs during stress corrosion cracking (SCC) in FCC alloys, which have a ductile behaviour in air (Magnin and Gras (1)). Different models were proposed some years ago, principally based on the interactions between corrosion (anodic dissolution and hydrogen effects) and plasticity. Nevertheless, none of them can give predictive laws, because of the extreme localization of the involved mechanisms. Numerical simulations at the scale of the dislocations can be of particular interest in this field. One of these models, the corrosion enhanced plasticity model (CEPM), was proposed to describe the SCC of austenitic stainless steels (2). It can be extended to pure metals with an increasing stacking fault energy (SFE), such as copper. The aim of this paper is (i) to present the experimental results of SCC in copper single crystals, (ii) to discuss new developpements of the model and (iii) to present the first results of a numerical simulation of the corrosion-dislocation interactions at a crack tip.

* Ecole des Mines de Saint Etienne, Centre SMS, URA CNRS 1884

SCC BEHAVIOUR OF <100> COPPER SINGLE GRYSTALS

Experimental.

Square cross section single crystals of pure copper were tested under slow strain rate in an 1M $NaNO_2$ solution at free potential. The <100> orientation of the crystals was chosen to get the average {100} macroscopic plane in favorable conditions for cracking and to look if the macroscopic cracking is achieved by microcracking involving {111} slip planes as in the CEPM. This model invokes the localization of stress concentrations, due to the formation of dislocation pile-ups. Such pile-ups are observed in materials with a small SFE value, which promotes planar glide and the presence of strong obstacles such as Lomer locks. Copper is an unfavorable case for the model because of its intermediate SFE (50 mJ/m^2). Indeed, there is a cellular arrangement of dislocations at the crack tip in the absence of a corrosive environment, as shown by Meletis et al (3). And because of its purity (99.999 %), precipitates cannot be invoked as obstacles to the dislocations motion. Copper is known to be sensitive to SCC in $NaNO_2$ solutions below a critical strain rate value. So, tests were performed at $\dot{\varepsilon}=10^{-7}\ s^{-1}$.

Results.

Figure 1a illustrates the macroscopic crack surface. Under these conditions, copper becomes macroscopically brittle, showing fracture planes separated by river lines, which is very surprising for such a ductile material. The elongation to rupture is about 10 %, compared to 50 % in air. Crack initiates on the right side and propagates to the left, with a macroscopic crack front in the <110> direction, parallel to the external surface. Figure 1b shows a detail of the crack surface. The average plane between two rivers and the macroscopic propagation direction are actually achieved by two symetrical systems of discontinuous zigzag microcracking. The direction of the parallel arrest lines between two succesive microfacets were determined for each system, by matching up their projections in different planes when tilting the sample in the microscope. They were found to be of <112> type. This corresponds to the intersection between {111} (light) and {110} microfacets (dark).

Considering the best orientation for cracking and the decohesion energy, the {110} planes are in the most favorable conditions for decohesion. But no microcracking along alternate {110} facets could achieve the observed propagation direction. Furthermore, the {111} facets are common to the two fracture systems and contains the macroscopic crack front. This means that they lead to impose the macroscopic propagation direction. Thus, the key question is related to the nature of a complex fracture mechanism, involving the slip planes, which causes their decohesion.

THE CORROSION ENHANCED PLASTICITY MODEL

This model is based on the softening effect due to corrosion localized at the crack tip, as shown by Magnin et al (4). It takes into account the generation of vacancies and hydrogen due to localized anodic dissolution and film formation. The following steps are considered (figure 2) :

1 - Slip planes activated at the very crack tip depassivate the metal and a localized dissolution takes place on these {111} planes.
2 - Corrosion produces a localized plasticity enhancement on these {111} planes. More mobile dislocations are injected because of vacancy production (anodic dissolution) and because of hydrogen absorption. Blunting is then reduced. Thus the role of corrosion is essential but indirect, by enhancing the plasticity at the very crack tip.
3 - Further from the crack tip, emitted dislocations will interact with obstacles present in the previously hardened zone formed when the stress is applied. Two zones will be considered along the slip plane : an enhanced plasticity zone near the surface blocked by a previously hardened zone. This will induce the formation of pile-ups where the local stress will increase.
4 - If the obstacles are strong enough, local k_{IC} can be reached, particularly if it is lowered by absorption of hydrogen. A crack's embryo will form by a kind of Stroh mechanism.
5 - Hydrogen lowers the decohesion energy of the {111} microfacets and the normal stress can be sufficient to open the crack along the slip plane. Dislocations are emitted on an asymetrical plane, shielding the new crack tip. Depending on the cristallographic orientation, cracking can occur on {111} or {110} facets.
6 - This process is expected to lead to regular changes of crak planes. A zigzag microcracking can occur, involving {111} planes.

The key question is related to the strength of the pile-up and the nature of the obstacles in pure copper. Strong pile-ups are usually not possible in materials with quite large value of the SFE, but it was shown that corrosion promotes a planar glide at a stress corrosion crack tip (3). Furthermore, because of the absence of strong obstacles in pure copper and because of the straight and regular aspect of the arrest lines, classical obstacles cannot be invoked. One can think about a kind of mobile obstacle corresponding to the interface between the diffusion zone (enhanced plasticity) and the previously hardened zone. Thus, strong individual obstacles are not needed, but the mobile dislocations are pinned by the forest in the hardened zone. One can understand how the edges can be so straight (figure 2), corresponding to the shape of the diffusion front, and how the facets can be regular, corresponding to a maximum distance of diffusion as a function of time.

NUMERICAL SIMULATION OF THE CEPM

Simulation method.

The situation simulated is shown on figure 3 and adapted to the cristallography observed in figure 1b. Calculations are made in two dimensions on straight edge dislocations emitted on a slip plane from the crack tip which is parallel to a <112> direction (intersection between the {111} and {110} facets). The angle between the slip plane and the average crack plane is about 35°, to fit with the observed macroscopic fracture surface orientation. The hardened region is modelized by a forest of punctual obstacles in the slip plane (Lomer locks for instance), which pin the emitted dislocations. The possibility for a dislocation to move is related to its line tension, the local stress and the resistance of the obstacles (figure 3), which is estimated through the classical relation for hardening. A diffusion zone of vacancies and hydrogen produced by the electrochemichal reactions at the crack tip is introduced along the slip plane and get a sequential advance. In the diffusion zone, the resistance of the obstacles is neglected, simulating the effects of corrosion on the enhanced mobility of the dislocations.

During the calculation, dislocations are emitted at a distance 2b (Burgers' vector) from the crack tip. At every sequence of the diffusion advance, all the dislocations in the slip plane move until they get a stable position. The local stress applied on a dislocation is determined using the formulation proposed by Lin and Thomson in the general case (5). It is related to the applied stress, the image force and the interactions with other dislocations in the slip plane. A simplified expression in pure mode II for an edge dislocation i can be written as :

$$\sigma_i = \frac{K_{II}}{\sqrt{2\pi i}} - \frac{\mu b}{4\pi(1-\nu)} + \frac{\mu b}{2\pi(1-\nu)} \sum_{\substack{k=1 \\ k \neq i}}^{n} \frac{1}{x_i - x_k} \sqrt{\frac{x_k}{x_i}}$$

where K_{II} is the stress intensity factor, x_i the distance of the dislocation form the crack tip and n the number of dislocations in the slip plane.

Results.

Figure 4 shows sequences of the computer simulation. The plane of the figure is the slip plane. The diffusion zone is in light grey, the hardened zone in black, the dislocations in white. The formation of a pile-up occurs at the diffusion front. When the diffusion zone gets a sequence of advance, it breaks the stable configuration of the pile-up and dislocations move to pile-up again on the new position of the diffusion front. There is a competition between the stability of the pile-up and the diffusion advance, simulating the mobile obstacle. The applied stress (σ_a) and the stress calculated in front of the pile-up (σ_i) are shown. The

stress concentration at the crack tip is transfered to the moving obstacle, where hydrogen can promote a brittle decohesion. A calculation made for a fixed obstacle shows another effect of hydrogen. Indeed, it segregates on edge dislocations and lowers their interactions, as shown by Sofronis and Birnbaum (6). The dislocation density is shown to increase strongly at the head of the pile-up, which increases the hydrogen concentration on the slip plane and then the embrittlement effect.

CONCLUSION

Copper exhibits a brittle behaviour in SCC, with a discontinuous cleavage-like fracture. The new notion of a mobile obstacle to the dislocation motion is able to explain this behaviour in the absence of more classical fixed obstacles. The numerical modelling of this moving interface is quite relevant. Quantitative estimation of the possible fracture mechanisms is possible. Further studies will deal with the effects of strain rate and temperature on the competition between the pile-up formation and hydrogen diffusion, by introducing laws for dislocation dynamics and diffusion kinetics.

REFERENCES

(1) Magnin T. and Gras J.M., Corrosion-Deformation Interactions, les Editions de Physique, 1992.

(2) Magnin T., Chierragatti R. and Oltra R., Acta. Met., Vol. 38., No 7, 1990, p. 1313.

(3) Meletis E.I., Lian K. and Huang W., Corrosion-Deformation Interactions, les Editions de Physique, 1992., p. 69.

(4) Magnin T., Chambreuil A. and Chateau J.P., accepted by Int. Jour. of Frac., 1996.

(5) Lin J.H. and Thomson R., Acta. Met., Vol. 34, No 2, 1986, p. 187.

(6) Sofronis P. and Birnbaum H.K., internal report, 1994.

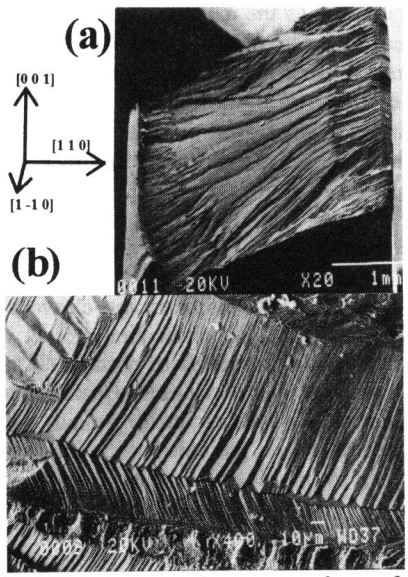

Figure 1 : SCC fracture surface of <100> pure copper single crystals.

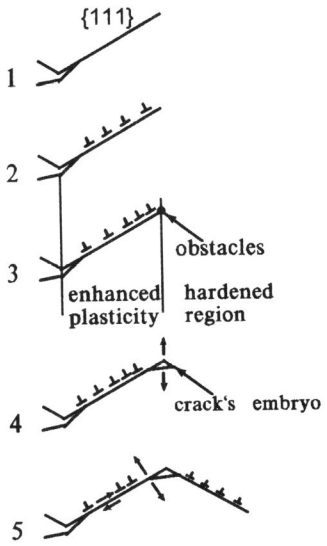

Figure 2 : Schematization of the corrosion enhanced plasticity model.

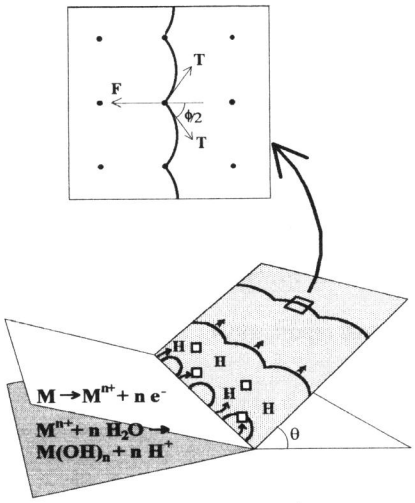

Figure 3 : Simulated situation at the SCC crack tip.

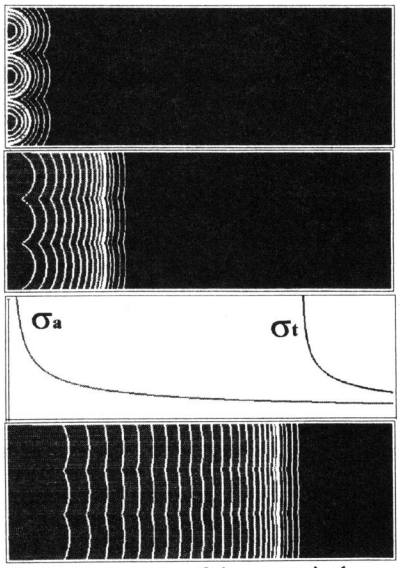

Figure 4 : Results of the numerical simulation of the CEPM for copper.